

General Disclaimer

One or more of the Following Statements may affect this Document

- This document has been reproduced from the best copy furnished by the organizational source. It is being released in the interest of making available as much information as possible.
- This document may contain data, which exceeds the sheet parameters. It was furnished in this condition by the organizational source and is the best copy available.
- This document may contain tone-on-tone or color graphs, charts and/or pictures, which have been reproduced in black and white.
- This document is paginated as submitted by the original source.
- Portions of this document are not fully legible due to the historical nature of some of the material. However, it is the best reproduction available from the original submission.

NDE for Heat Engine Ceramics

(NASA-TM-86949) NDE FOR HEAT ENGINE
CEMAMICS (NASA) 13 p HC A02/HF A01 CSCL 14B

N85-20389

G3/38 Unclass
14419

Stanley J. Klima
Lewis Research Center
Cleveland, Ohio



**Prepared for the
Twenty-second Automotive Technology Development
Contractors' Coordination Meeting (ATD/CCM)
sponsored by the Society of Automotive Engineers
Dearborn, Michigan, October 29–November 2, 1984**



ABSTRACT

Radiographic, ultrasonic, and scanning laser acoustic microscopy (SLAM) techniques were used to characterize silicon nitride and silicon carbide MOR bars in various stages of fabrication. Conventional and microfocus x-ray techniques were found capable of detecting minute high density inclusions in as-received powders, green compacts, and fully densified specimens. Significant density gradients in sintered bars were observed by radiography, ultrasonic velocity, and SLAM. Ultrasonic attenuation was found sensitive to microstructural variations due to grain and void morphology and distribution. SLAM was also capable of detecting voids, inclusions, and cracks in finished test bars. It was determined that thermoacoustic microscopy techniques have promise for application to green and densified ceramics. Some limitations and the detection probability statistics of the aforementioned NDE processes are also discussed.

THE INCREASED FUEL EFFICIENCY resulting from higher allowable engine operating temperatures makes structural ceramics such as silicon nitride and silicon carbide attractive candidate materials for hot section components in advanced heat engines. These materials have excellent oxidation and thermal shock resistance and good average high temperature strength. However, current structural ceramics also exhibit wide scatter in strength and relatively low fracture toughness. Poor mechanical properties are generally attributed to defects generated during fabrication (1).^{*} Component reliability can be improved by screening out defective parts through nondestructive evaluation (NDE). There also exists the possibility of

^{*}Numbers in parentheses designate references at end of paper.

reducing the cost of fabrication by utilizing NDE techniques in the early stages of processing to avoid the expense of finishing rejectable parts. Perhaps even more importantly, if NDE techniques were incorporated into a ceramic materials technology development program, information might be obtained regarding the source of defects and steps could be taken to minimize their occurrence through improved fabrication methods. Thus, NDE has the potential for helping to reduce the effort expended in a materials research program and shorten the time needed to develop reliable structural ceramics. It is with these reasons in mind that a program for NDE of ceramics was established to provide direct support to the recently expanded ceramic materials development effort at the NASA Lewis Research Center.

The objectives of the NDE program are to identify and develop conventional and newly emerging methods for application to ceramics research materials and heat engine components as well as to establish NDE methodology for ceramics process control, properties verification, and degradation assessment. The following sections are essentially a review of the Lewis program. Pertinent results and observations are presented but technical details are minimized for the sake of brevity.

MATERIALS PROCESSING AND NDE

Figure 1 contains a simplified flow chart which illustrates the integration of NDE into the ceramics materials technology development program. The as-received powders were procured commercially and mixed with suitable sintering aids/binders and milled to provide a uniform mix and reduce the particle size. Green test bars were prepared from the resulting mix by die pressing followed by isopressing. After the sintering operation, the densified bars were diamond ground to final dimensions which measured, nominally, 3.0 by 0.60 by 0.28 cm. A detailed description of the fabrication procedure is given in Ref. 2. The test bars

were ultimately tested to fracture in four point bending.

Although a wide variety of NDE methods are available for application to fully densified ceramics, the highly porous nature of the materials in the green state limits the number of useful techniques to those which are noncontacting or noninvasive in nature. Introduction of foreign material, for example a liquid ultrasonic couplant, into the pores could result in adverse sintering effects which would in turn result in lower material strength. Of the few applicable noncontacting techniques, x-ray radiography is the most highly developed and is relatively fast and easy to apply. Both conventional and microfocus techniques were utilized in this program for detection of discrete voids, foreign particles, and density variations at all stages of processing. Another recently developed technique called photoacoustic microscopy is emerging as a possible noncontacting method for evaluating ceramics. Although it is not as fast as radiography the indication is that it may have much greater sensitivity to flaws less than 100 μm in size. An effort to develop this technique for application to ceramics in the green as well as the densified state has been initiated.

Ultrasonic techniques were also used to evaluate fully densified specimens for detection of discrete defects as well as density and microstructural variation.

RADIOGRAPHY

X-ray methods were used to evaluate ceramic materials in all stages of specimen fabrication. Figure 2 shows reproductions of film radiographs of MOR bars selected from a single batch of silicon nitride. The radiographs exhibit significant variations indicative of bulk density gradients in the specimens after firing. The variations are caused by differences in x-ray absorption, which is directly proportional to the number of atoms encountered by the x-ray beam passing through the material. Dimensional effects in these bars were eliminated by diamond grinding all specimens to a uniform thickness before the x-rays were taken. Thus, the darkest regions on the radiographic prints represent zones of highest material density while the lighter shades of gray indicate zones having proportionally lower density. The images provide excellent qualitative information on the nature of density variations within and among specimens. Characteristically, all bars except for the one on the left side of Fig. 2 contain a low density core surrounded by a relatively high density case. The case-core configuration appeared to be unique to each specimen, so much that the radiographs were frequently used to confirm specimen identification. The observed density variations appeared to be related to temperature gradients, specimen position, and spacer contact area in the sintering furnace.

Availability of the radiographic information regarding density fluctuations made it possible to correct problems in the sintering operation and produce more uniform specimens earlier in the program than would otherwise have been possible had

x-rays not been utilized as a quality control tool. Figure 3 contains radiographs of four pairs of MOR bars, each sintered under a different set of conditions. It is evident from the bulk density measurements as well as from the radiographs that densification was affected by both time at temperature and the way in which the specimens were separated from each other during firing. For example, after 1 hr at 2140 °C, the specimens separated by BN disks (minimum contact area) had a bulk density 4 percent higher than the specimens separated by a thin layer of BN powder. The difference appears to be primarily in the extent of the low density core as evidenced by radiographs of both specimen pairs. On the other hand, the specimens sintered for 1 hr in minimum contact with disk spacers had the same bulk density as specimens sintered for 4 hr in full contact with disk spacers. The radiographs show, however, that the former exhibit a low density core while the latter appear to have relatively uniform density distribution over the entire specimen. Also, specimens sintered for only 2 hr in full contact with BN disks had a relatively uniform density distribution and only slightly lower bulk density. It should be noted that the information presented here is not sufficient to draw conclusions regarding optimized sintering conditions for silicon nitride. It does show, however, that radiography can be used to advantage for development of better fabrication/processing techniques.

The x-ray technique was also used to detect foreign particles, particularly those with relatively high density compared to silicon nitride and silicon carbide. The x-ray absorption coefficient varies directly as a function of atomic number, therefore the greater the difference between the foreign particle and the matrix material, the greater the film contrast on the radiograph, and generally the smaller the particle that can be imaged. Figure 4 presents radiographs of a single MOR bar taken after three stages of processing. All three radiographs contain tiny dark spots which represent the location of high density inclusions. Particular attention should be given to two prominent inclusions just to the right of center of the specimen. These particles persisted throughout the fabrication cycle with little or no modification during firing and were sufficiently deep that they were not removed by surface grinding of the test bar.

The specimen contains a greater number of high density particles in the green state than in the as-fired condition. This suggests that many of green state inclusions may consist of agglomerates of oxides that were added to aid the densification process. During sintering, the oxides (e.g., Y_2O_3 and SiO_2) contribute to the formation of a glassy phase which becomes diffuse and can no longer be detected by x-rays. Some defects also disappear after surface grinding. For example, the number 2 was inscribed in the surface of the green specimen after pressing to identify it as being from batch two. The number shows up as a white object because the inscription is essentially a curvilinear void. The number is also seen in the radiograph made after firing but

note that both the number and the specimen dimensions have shrunk significantly due to material densification. After surface grinding of course, the batch number is no longer visible in either the radiograph or the specimen.

Some inclusions found in green compacts were analyzed after sanding off outer layers of specimen material to bring the particle to the surface. The compositions of typical heavy density inclusions are listed in the table of Fig. 4. Iron was most frequently encountered while other materials such as tin and nickel base alloy particles were uncommon. One particle was identified as Ce rich, indicating that it may be an agglomerate of Ce_2O_3 which was used as a sintering aid in that specimen. Although it is suspected that many such oxide agglomerates exist, they are very difficult to locate for analysis because their physical appearance is very much like the matrix and therefore difficult to identify visually. The particle sizes listed in the table are typical of the few particles that were analyzed and do not necessarily represent the smallest detectable size.

Samples of as-received powder were also radiographed to determine if any foreign particles were present prior to in-house processing. Figure 5 shows radiographs of lightly compacted disks which contain numerous high density particles indicating that, other than the oxide additives, most high density inclusions originated during production of the starting powders. Thus the methods of producing ceramic starting powders must be improved or some method for removing foreign particles must be devised to clean up the powder before making green compacts.

SCANNING LASER ACOUSTIC MICROSCOPY

The scanning laser acoustic microscope (SLAM) was used for detection of surface and near surface defects as well as for revealing patterns of density variations. Figure 6 contains two amplitude mode acoustic micrographs showing three types of defects in silicon nitride. Flaw A is a surface connected inclusion about 75 μm in diameter. The same inclusion was detected by x-rays as a high density particle and, since it was surface connected, it could also be seen optically at magnifications of $\times 10$ to $\times 30$. Flaw B is a planar crack-like defect which is also surface connected and could be seen optically. However, it was not detected by x-rays because it is essentially two-dimensional and therefore could not be resolved on the radiograph. Flaw C is also a crack-like feature but is situated beneath the surface. Although it was easily detected by the SLAM, it could not be resolved by either radiographic or optical methods. In addition to the discrete defects just described, the SLAM images also exhibit a background consisting of long straight linear indications caused by diamond grinding grooves, and small ripples not associated with any obvious feature. It is probable that the tiny ripples are caused by microstructural features which disturb the general sound field but are too small and too numerous to be resolved individually. More work is required to determine the

nature of these very small scattering sites and what relationship they may have to ceramic material properties.

Scanning laser acoustic microscopy can also be used in the interference mode (3) to obtain information regarding bulk density variations. In a specimen with constant thickness, the time of travel of an ultrasonic wave provides a measure of sound velocity, and velocity can be used to infer material density (4). SLAM interferograms can be used to image velocity variations that occur within the viewing field as shown in Fig. 7. Any deviation in time of travel will cause the interference lines to bend to the right or left. The relatively straight lines in Fig. 7(a) imply that, within the field of view (2.75 by 2.0 mm), the density of the ceramic specimen is relatively uniform. In Fig. 7(b) however, the density at the bottom (near the edge of the MOR bar) is significantly greater than at the top of the image which is located a little over 2 mm away from the specimen edge. These observations agree with those made on the radiographs shown previously.

ULTRASONIC VELOCITY AND ATTENUATION

Ultrasonic velocity and attenuation measurements were used to characterize density and microstructure in monolithic silicon nitride and silicon carbide. Research samples exhibiting a wide range of density and microstructural variations were used to demonstrate that bulk density variations correlate with and can be estimated by velocity measurements (Fig. 8). Variations in microstructure (grain size and shape or void size and distribution) in silicon carbide had only a slight effect on velocity (4). Similar measurements were also made on silicon nitride samples containing a low density core surrounded by a high density case, as well as on uniformly dense specimens (Fig. 9). The velocity for each bar is the average of three measurements over the specimen length. Just as for silicon carbide, the average ultrasonic velocity for these specimens increases with increasing density. There is a 6 percent difference in both density and velocity between the top and bottom specimens in Fig. 9. However, while the specimen in the middle is 3 percent less than the one on top, the velocity is only about 1 percent less. This suggests that in specimens containing steep density gradients such as these, a large number of velocity measurements, each on a relatively small sample volume, should be made for precise quantitative material characterization. Thus, the materials could be scanned to produce an accurate map of velocity and hence density as a function of position on the sample.

Although significant variations in certain microstructural features had only a slight effect on ultrasonic velocity it was found that the same variations had a profound effect on attenuation of high frequency ultrasonic waves. Figure 10 shows a plot of attenuation as a function of ultrasonic frequency for some of the same specimens used in the velocity-density study. Eight silicon carbide samples, all with similar bulk densities were selected. The specimens were

divided equally into sets with two widely differing microstructures as shown in Fig. 10. The plot shows that attenuation in the large grained material is at least four times higher than for the small grained material. Although the grain size is the most obvious microstructural difference between the two sample groups, there also exist other features that could affect ultrasonic attenuation. For example, the less attenuating material has equiaxed grains while many grains in the more attenuating material are elongated or rod-like in shape. The void size and morphology is also quite different. Although the total porosity is the same for the two sample groups as evidenced by the measured bulk density, the photomicrographs show that voids are larger but fewer in number in the more attenuating material. It is probable that all of the variations in microstructure just described have a cumulative effect on total measured attenuation in the ceramic samples. It is not clear which feature has the greatest effect at this time because the variables could not be separated, something that is difficult to do during thermomechanical processing of the materials.

Modulus of rupture test results from the samples show that the material with the fine microstructure is significantly stronger at room temperature than the coarser material. This suggests that ultrasonic attenuation measurements may be useful as a quality control tool to assure material strength to the extent that it is controlled by microstructure. More work is needed in this area.

FRACTURE MECHANICS AND NDE RELIABILITY

The reliability of an NDE procedure is defined as the efficiency of that procedure in detecting flaws of a specific type and size. After nondestructive examination it cannot be said that a particular component is entirely free of flaws simply because none were found; it can only be asserted that there is a certain probability that the part is free of defects of a specific type and size (5). The higher the level of this probability, the higher the reliability of the NDE procedure and therefore the higher the reliability of the part that was inspected.

The need for quantitatively assessing the reliability of flaw detection has arisen from the application of fracture mechanics principles to the design of critical parts. The fracture mechanics concept assumes that flaws will exist and then quantitatively describes their effect on strength. Thus, a critical crack size is defined for a particular material and loading condition. The role of NDE is to assure that flaws corresponding to the critical crack size for fracture at the design load are absent when the part is put into service. Furthermore, it may be necessary to guarantee that flaws much smaller than the critical size are absent to account for possible subcritical crack growth, especially where stress corrosion cracking or fatigue loading may be encountered.

The use of fracture mechanics concepts places a premium on the ability of nondestructive

inspection to detect small defects, and on the need to determine the practical reliability of a particular NDE procedure when that procedure is used to detect flaws of a specific type and size. If the design is such that the critical crack size based on design loads is greater than the smallest flaw that can be reliably detected, the inspection process can be used. The difference between the critical size and the smallest detectable size is a measure of the factor of safety.

An example of NDE reliability data developed for two x-ray techniques, according to the guidelines set forth in Ref. 5, is presented in Fig. 11 in the form of a plot of probability of detection as a function of void size. The curves define the lower limit of probability of detection (a conservative estimate) calculated at a confidence level of 95 percent using the binomial distribution. Details are given in Ref. 6. The significance of this type of data is that it provides information regarding the flaw size that can be detected with a reasonable degree of reliability. For example, the curve for microfocus radiography shows that the probability of detection is 90 percent or higher for void diameters equal to or greater than 1.5 percent of specimen thickness. For conventional radiography similar probabilities of detection are indicated only for voids exceeding 2.5 percent of specimen thickness. The plots also show that smaller voids can sometimes be detected but with lower detection reliability. The designer can now utilize this type of data to determine the largest flaw that will be missed a significant proportion of time, and take steps to ensure that operating stresses are adequate to prevent that size flaw from becoming critical. Very little data of this type exists today. Too often, the smallest detectable flaw sizes are reported for specific techniques with no regard to the probabilistic nature of the NDE process.

THERMOACOUSTIC IMAGING

Like the x-ray technique, thermoacoustic imaging can be used in a noncontacting, noninvasive mode. Commonly referred to as photoacoustic microscopy, photoacoustic spectroscopy, or thermal wave imaging (7-10), the technique essentially measures relative differences in surface and near-surface thermal properties of the material being evaluated. The absorption of intensity modulated electromagnetic radiation focused at any point on the sample gives rise to localized cyclic heating and cooling which generates sound waves. The amplitude and phase of these waves can be measured at another point on the specimen surface with a piezoelectric crystal or in the surrounding medium by a sensitive microphone. Thermoacoustic waves are commonly generated by absorption of laser light or an electron beam but other forms of electromagnetic energy such as microwaves, infrared, or x-rays might also be used. Laser methods are also being considered for picking up signals (10). This adds to the versatility and flexibility of the thermoacoustic technique.

A study is under way to further develop and define the capabilities of the method for appli-

cation to structural ceramics for heat engine applications. The specific goals are to detect voids 10 μm and larger at depths ranging up to 1 mm, to develop a capability for detecting surface-connected cracks 15 μm long, 5 μm deep, and 1 μm wide, and to predict failure sites on MOR bars as well as to obtain strength correlations.

CONCLUDING REMARKS

Our investigation showed that radiography is an essential tool for NDE of ceramics. Because the method is noncontacting and noninvasive, x-rays can be used at all stages of fabrication to detect steep density gradients, and volumetric flaws such as high density inclusions and oxide agglomerates, as well as discrete voids. The probability of detection of voids was higher for microfocus x-ray techniques than for conventional methods but the conventional methods are faster. Radiographic sensitivity to volumetric flaws is excellent, providing the x-ray absorption coefficient of the flaw is not similar to the matrix material, as in the case of loose agglomerations of matrix powder particles. The sensitivity to cracks is poor unless the plane of the crack is aligned with the direction of the x-ray beam and the crack is not tight (tight cracks have essentially no volume).

Scanning laser acoustic microscopy was useful for detecting surface and near surface defects in densified ceramics. Unlike radiography the technique is capable of detecting both volumetric and crack-like flaws. The sensitivity to tight cracks is good except when the plane of crack is aligned in the same direction as the ultrasonic beam. (The orientation that is worst for radiography is best for ultrasonics.) Surface finish is important for flaw detection since as-fired surfaces present a much higher background noise level than diamond ground or polished surfaces. The probability of detection can be significantly different for each condition. Ceramics with a high level of porosity (densities less than 80 percent of theoretical) also present a problem because the large number of pores scatter the sound waves. In the interference mode the SLAM can also provide a qualitative indication of density variations by virtue of the effect on ultrasonic velocity.

Ultrasonic velocity and attenuation measurements were determined to be useful for characterizing ceramics in terms of density and microstructure. Bulk densities of silicon nitride and silicon carbide correlate with and can be estimated by velocity measurements. Although

variations in certain microstructural features had only a minor effect on velocity they had a strong effect on ultrasonic attenuation. It appears that attenuation measurements may be capable of estimating material strength to the extent that it is determined by microstructure.

REFERENCES

1. H.K. Bowen, et al., "Basic Research Needs on High Temperature Ceramics for Energy Applications." *Materials Science and Engineering*, Vol. 44, 1980, pp. 1-56.
2. W.A. Sanders, and D.M. Mieskowski, "Strength and Microstructure of Sintered Si N With Rare Earth Oxide Additions." *American Ceramics Society Bulletin*, Vol. 64, No. 2, Feb. 1985, pp. 304-309.
3. L.W. Kessler, D.E. Yuhas, and C.L. Vorres, "Acoustic Microscopy of Ceramics." in *Proceedings of The DARPA/AFWAL Review of Progress in Quantitative NDE*, AFWAL-TR-81-4080, Sept. 1981, pp. 128-135. (AD-A108741.).
4. S.J. Klima, G.K. Watson, T.P. Herbell, and T.J. Moore, "Ultrasonic Velocity for Estimating Density of Structural Ceramics." *NASA TM-82765*, Oct. 1981.
5. P.F. Packman, S.J. Klima, J. Malpani, J. Moyzis, W. Walker, B.G.W. Yee and D.P. Johnson, "Reliability of Flaw Detection by Nondestructive Inspection." in *Metals Handbook*, 8th Edition, Vol. 11, Edited by H.E. Boyer, American Society for Metals, Metals Park, OH, 1976 pp. 414-424.
6. G.Y. Baaklini, J.D. Kiser, and D.J. Roth, "Radiographic Detectability Limits for Seeded Voids in Sintered Silicon Carbide and Silicon Nitride." *NASA TM-86945*, 1984.
7. A. Rosencwaig, and A. Gersho, "Theory of the Photoacoustic Effect with Solids." *Journal of Applied Physics*, Vol. 47, No. 1, Jan. 1976, pp. 64-69.
8. Y.H. Wong, R.L. Thomas, and G.F. Hawkins, "Surface and Subsurface Structure of Solids by Laser Photoacoustic Spectroscopy." *Applied Physics Letters*, vol. 32, No. 9, May 1978, pp. 538-539.
9. A. Rosencwaig, "Photoacoustic Microscopy." *American Laboratory*, vol. 11, No. 4, Apr. 1979, pp. 39-40, 42, 47-49.
10. R.L. Thomas, L.D. Favro, P.K. Kuo, D.N. Rose, D. Bryk, M. Chaika and J. Patt, "Scanning Photoacoustic Microscopy of Aluminum with Aluminum Oxide, Roughness Standards and Rubber." *U.S. Army Tank-Automotive Command, TACOM-TR-12957*, June 1984.

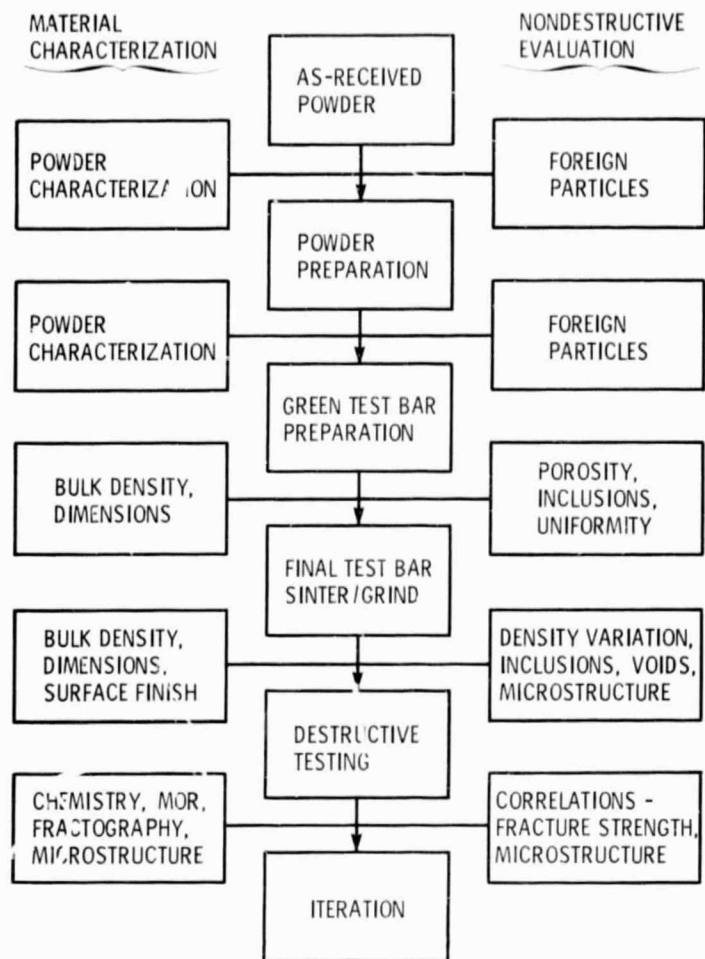


Figure 1. - Integration of NDE into a ceramic materials development program.

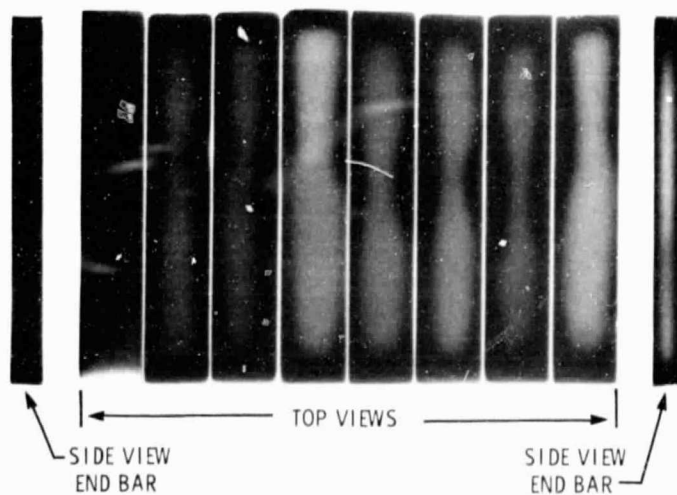


Figure 2. - Radiographs of MOR bars showing density variations within a single batch of sintered silicon nitride. The specimens were ground to a uniform thickness.









THRU-THICKNESS RADIOGRAPH	SINTERING TIME AT 2140 °C	SPECIMEN SPACERS	MEAN BULK DENSITY, G/CC
	1 HR	BN DISK MIN CONTACT	3.17
			3.18
	4 HR	BN DISK FULL CONTACT	3.17
			3.17
	2 HR	BN DISK FULL CONTACT	3.16
			3.14
	1 HR	BN POWDER FULL CONTACT	3.03
			3.06

Figure 3. - Illustration of the use of X-rays to monitor densification of silicon nitride MOR bars sintered under various conditions. Radiographs show how different combinations of time-at-temperature and specimen spacer arrangement can alter material density distribution.




		
GREEN COMPACT (ISOPRESSED)		
	REPRESENTATIVE INCLUSIONS DETECTED AND ANALYSED	
AS-FIRED MOR BAR	TYPE	SIZE, % THICKNESS
	Fe	0.5
	Sn	0.5
	Ni, Cr, Co, Ti	1.3
	Ce rich	1.5
MOR BAR AFTER GRINDING		

Figure 4. - Illustration of the use of radiography to detect and monitor high density foreign particles throughout the fabrication process. Chemical analysis was performed on selected samples taken from the green silicon nitride compacts.

ORIGINAL PAGE IS
OF POOR QUALITY.



Figure 5. - Radiographs of as-received Si₃N₄ powder showing high density inclusions (dark specks). Disks were made by lightly compacting dry powder in a die at 56 MPa to a final thickness of 3 mm.

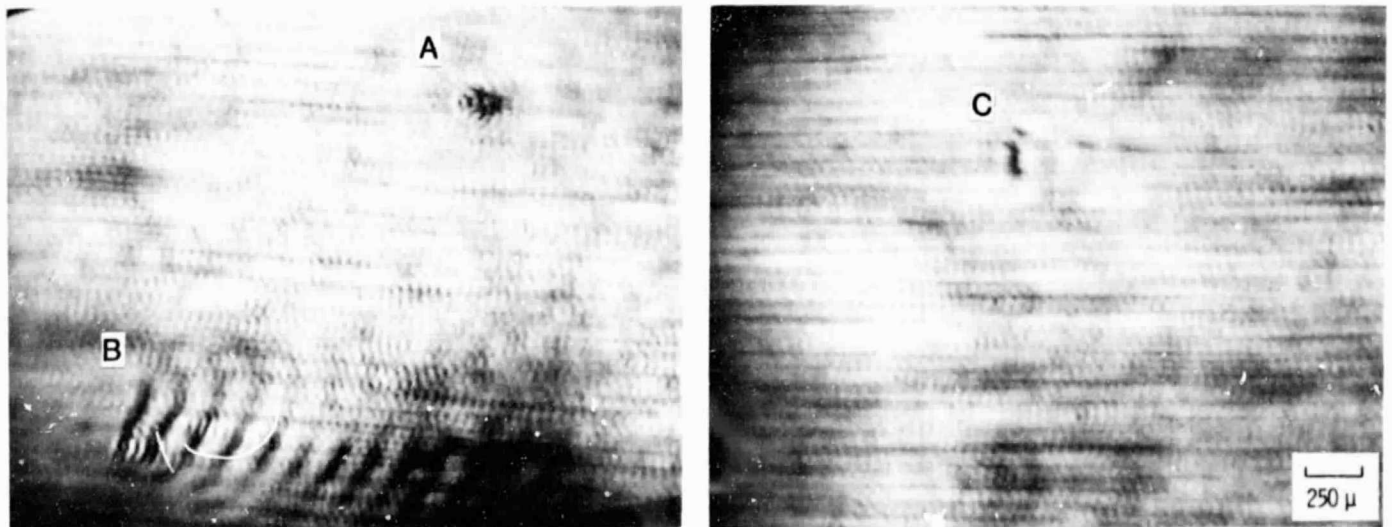
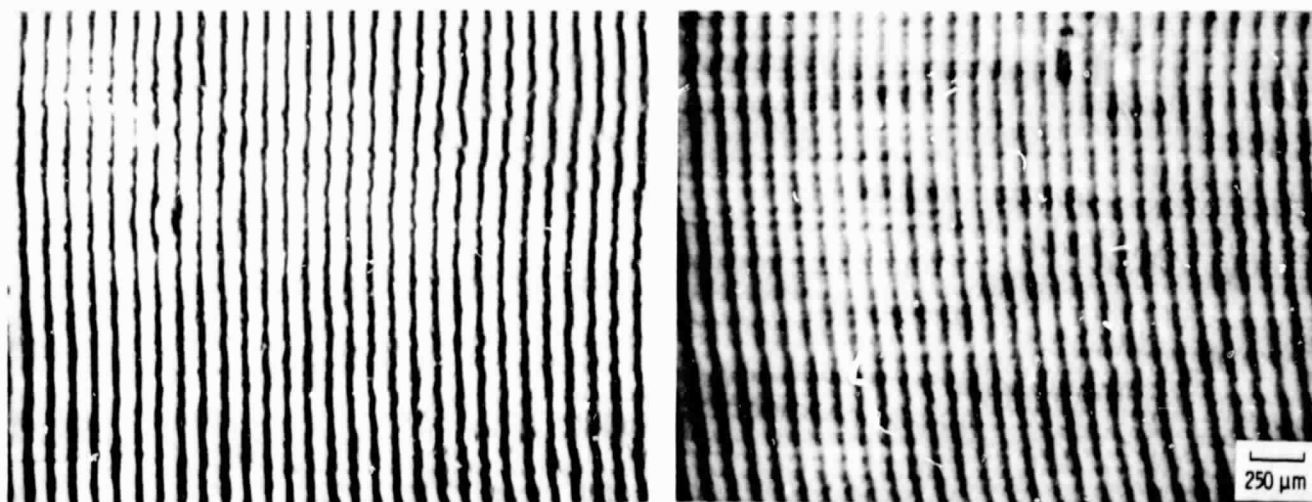


Figure 6. - Flaw images produced by scanning laser acoustic microscopy. (a) surface connected inclusion, (b) surface connected crack, (c) subsurface crack. Background shows images of grooves produced by grinding, and small ripples possibly caused by microstructural features.



(a) Density is essentially uniform.

(b) Density increases top to bottom.

Figure 7. - Interferograms produced by the scanning laser acoustic microscope illustrating a capability for imaging density gradients in Si_3N_4 MOR bars.

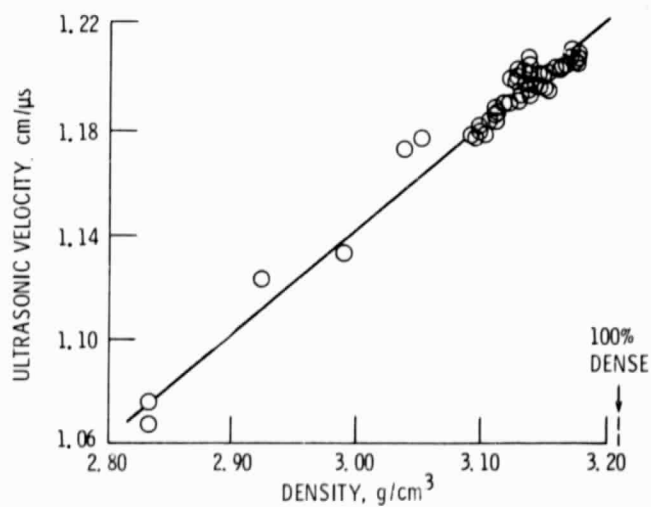


Figure 8. - Relationship between ultrasonic velocity and density of alpha silicon carbide. Data for material in as sintered and hot isostatically pressed conditions, and three grain sizes (Klima et al, 1981).




RADIOGRAPH	VELOCITY, cm/us	DENSITY, g/cc
	MEAN	MEAN
	1.1170	3.26
	1.1050	3.16
	1.0500	3.08

Figure 9. - Data from two NDE techniques provide complementary information regarding bulk density of sintered silicon nitride. Ultrasonic velocity is more quantitative but radiography can image density variations in greater detail.

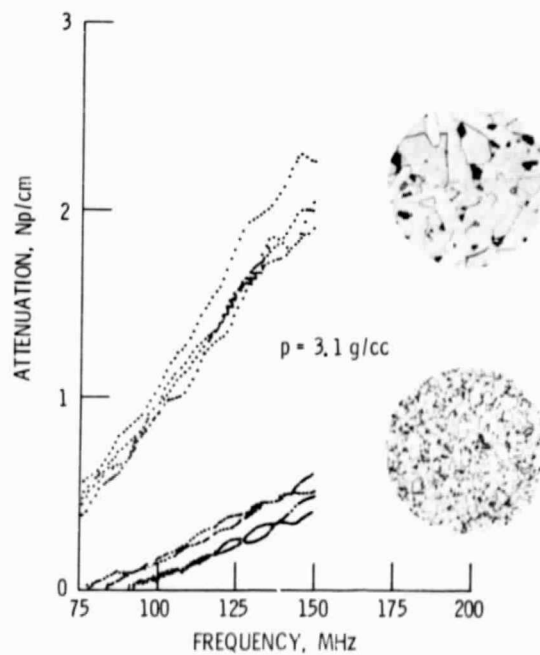


Figure 10. - Effect of microstructure on ultrasonic attenuation in sintered alpha silicon nit. ide.

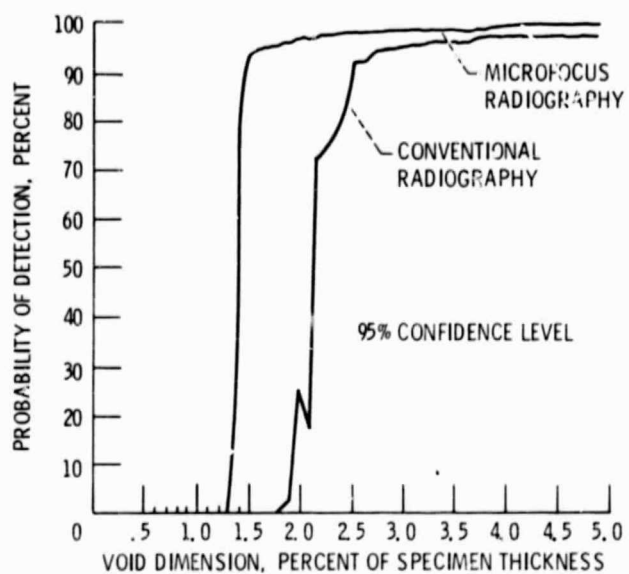


Figure 11. - Probability of detection of voids in sintered silicon nitride by X-ray techniques. Material is 99% of theoretical density (Baaklini, et al, 1985).